

Band Structure of White Tin*

MARIA MIASEK†

Department of Physics and Astronomy, University of Rochester, Rochester, New York

(Received 25 July 1962; revised manuscript received 26 December 1962)

A perturbation calculation of the band structure in white tin is performed using the orthogonalized plane wave approximation. The energies are determined for several points of high symmetry of the Brillouin zone for different choices of potential. On the basis of these results the properties of the Fermi surface in the neighborhood of these points are discussed. It is found that the first two Brillouin zones are completely filled with electrons.

I. INTRODUCTION

IN the last few years, extensive investigations of the band structure in polyvalent metals have been attempted, both experimentally and theoretically,¹⁻⁵ in order to establish the Fermi surface and the electronic properties of these metals. So far, there has been no attempt to find the band structure of white tin by theoretical calculations, though many attempts were made to establish its Fermi surface from experiment.⁶⁻¹⁴

Some papers on this subject are particularly important. One is that of Gold and Priestly⁸ dealing with the de Haas-van Alphen effect in white tin, where the authors gave the possible Fermi surface constructed for the free electron model. The other one is that of Alekseevskii *et al.*,⁹ where the open Fermi surface was found by consideration of the tetragonal symmetry and confirmed by galvanomagnetic measurements. Both investigations indicate that the Fermi surface is very complicated. The complexity of the Fermi surface is also confirmed by recent cyclotron resonance experiments,^{12,14} where 28 effective masses were found for white tin.

It, therefore, seemed to be of importance to try to

obtain some information on the band structure and Fermi surface in white tin from theoretical calculations. Until recently, it would have been difficult to perform any computation because there were no Hartree-Fock calculations for the tin atom. However, such calculations have now been performed by Herman and Skillman¹⁵ and quite independently by Mayers.¹⁶

From the form of the wave functions for 5s and 5p electrons, one sees at once that the conduction electrons in white tin cannot be treated as tightly bound. The 5s and 5p functions are so extended that the overlap integrals are very large. For example, the overlap integral ($ss\sigma$) computed for the nearest-neighbor distance has the value -0.2530 Ry. This corroborates the surmise, already well established from the studies of the band structure of the other polyvalent metals, that the band structure in white tin should not deviate very much from the free-electron model.

On this presumption it was decided to perform numerical calculations using the perturbation method in the orthogonalized plane wave (OPW) approximation, which in zero order describes the wave functions for the conduction electrons by single plane waves. This method has been described in papers of Bassani and Celli.¹⁷ In these first calculations on white tin, no attempt is made to work out the band structure in detail. Instead, by making some simplifying assumptions, energies at several points of high symmetry in Brillouin zone are computed.

II. SYMMETRY OF WHITE TIN

Here, a short description of the crystal structure of white tin is given. The white tin structure is considered here as a body-centered tetragonal with the lattice constants $a = 5.8197 \text{ \AA} = 10.9977a_0$, $c = 3.1749 \text{ \AA} = 5.9994a_0$, as shown in Fig. 1. It is the only centered tetragonal structure where the ratio $1/\mu = c/a = 0.5455$ is considerably different from unity. The basic primitive translations are: $\mathbf{a}_1 = (-a/2, a/2, c/2)$, $\mathbf{a}_2 = (a/2, -a/2, c/2)$, $\mathbf{a}_3 = (a/2, a/2, -c/2)$. The unit cell contains two atoms. The basis vectors for them are assumed to be (0,0,0) and

* This work was supported by the U. S. Air Force Office of Scientific Research.

† On leave of absence from the Institute of Theoretical Physics, University of Warsaw, Warsaw, Poland.

¹ *The Fermi Surface*, edited by W. A. Harrison and M. B. Webb (John Wiley & Sons, Inc., New York, 1960).

² V. Heine, Proc. Roy. Soc. (London) **A240**, 340, 361 (1957).

³ W. A. Harrison, Phys. Rev. **116**, 555 (1959); **118**, 1182, 1190 (1960); **126**, 497 (1962).

⁴ B. Segall, Phys. Rev. **124**, 1797 (1961).

⁵ L. M. Falicov, Phil. Trans. Roy. Soc. (to be published).

⁶ E. Fawcett, Proc. Roy. Soc. (London) **A232**, 519 (1955); Phys. Rev. **103**, 1582 (1956).

⁷ R. G. Chambers, Can. J. Phys. **34**, 1395 (1956).

⁸ A. V. Gold and M. G. Priestley, Phil. Mag. **5**, 1089 (1960).

⁹ N. E. Alekseevskii and Yu. P. Gaidukov, Zh. Eksperim. i Teor. Fiz. **37**, 672 (1959) [translation: Soviet Phys.—JETP **10**, 481 (1960)]; N. E. Alekseevskii, Yu. P. Gaidukov, I. M. Lifshitz, and V. G. Peschanskii, *ibid.* **39**, 1201 (1960) [translation: *ibid.* **12**, 837 (1961)]; N. E. Alekseevskii and Yu. P. Gaidukov, *ibid.* **41**, 1079 (1961) [translation: *ibid.* **14**, 770 (1962)].

¹⁰ T. Olsen and R. W. Morse, Bull. Am. Phys. Soc. **4**, 167 (1959).

¹¹ T. Olsen, Phys. Rev. **118**, 1007 (1960).

¹² M. S. Khaikin, Zh. Eksperim. i Teor. Fiz. **37**, 1473 (1959); **42**, 27 (1962) [translations: Soviet Phys.—JETP **10**, 1044 (1960); **15**, 18 (1962)].

¹³ A. F. Kip, D. N. Langenberg, B. Rosenblum, and G. Wagoner, Phys. Rev. **108**, 494 (1957).

¹⁴ A. F. Kip (private communication).

¹⁵ F. Herman and S. Skillman (private communication).

¹⁶ D. Mayers (private communication).

¹⁷ F. Bassani and V. Celli, Nuovo Cimento **11**, 805 (1959); Studia Ghisleriana **2**, 157 (1959); J. Phys. Chem. Solids **20**, 64 (1961).

TABLE I. Classification of s , p , and d states in the white tin structure.

Point Γ	8 one-dimensional representations 2 two-dimensional representations	Line ΓL	4 one-dimensional representations $\gamma = \exp(ik_x a/2)$
Γ_1^\pm	$2^{-1/2}(s\rangle \pm s\rangle_\tau)$	$(\Gamma L)_1, (\Gamma L)_2$	$2^{-1/2}(s\rangle \pm \gamma s\rangle_\tau)$
Γ_2^\pm	The s , p , and d functions do not form basis functions for Γ_2^\pm representations.		$2^{-1/2}(x\rangle \pm \gamma x\rangle_\tau)$
Γ_3^\pm	$2^{-1/2}(z\rangle \mp z\rangle_\tau)$		$2^{-1/2}(z\rangle \mp \gamma z\rangle_\tau)$
Γ_4^\pm	$2^{-1/2}(x^2 - y^2\rangle \pm x^2 - y^2\rangle_\tau)$	$(\Gamma L)_3, (\Gamma L)_4$	$2^{-1/2}(x^2 - y^2\rangle \pm \gamma x^2 - y^2\rangle_\tau)$
Γ_5^\pm	$2^{-1/2}(xy\rangle \pm xy\rangle_\tau)$		$2^{-1/2}(y\rangle \pm \gamma y\rangle_\tau)$
	$\begin{cases} 2^{-1/2}(x\rangle \mp x\rangle_\tau) \\ -2^{-1/2}(y\rangle \mp y\rangle_\tau) \end{cases}$		$2^{-1/2}(yz\rangle \mp \gamma yz\rangle_\tau)$
	$\begin{cases} 2^{-1/2}(xz\rangle \pm xz\rangle_\tau) \\ 2^{-1/2}(yz\rangle \pm yz\rangle_\tau) \end{cases}$		$2^{-1/2}(xy\rangle \pm \gamma xy\rangle_\tau)$
Point L	4 two-dimensional representations	Line ΓX	4 one-dimensional representations $\gamma = \exp(ik_x a/2)$
L_1	$\begin{cases} xy\rangle_\tau \\ xy\rangle \end{cases}$	$(\Gamma X)_1, (\Gamma X)_2$	$2^{-1/2}(s\rangle \pm \gamma s\rangle_\tau)$
L_2	$\begin{cases} s\rangle \\ s\rangle_\tau \end{cases}$		$2^{-1/2}(3z^2 - r^2\rangle \pm \gamma 3z^2 - r^2\rangle_\tau)$
L_3, L_4	$\begin{cases} - z\rangle_\tau \\ z\rangle \end{cases}$		$2^{-1}(x\rangle + y\rangle) \pm \gamma [x\rangle_\tau + y\rangle_\tau]$
	$\begin{cases} x^2 - y^2\rangle_\tau \\ x^2 - y^2\rangle \end{cases}$		$2^{-1}(xz\rangle - yz\rangle) \mp \gamma [xz\rangle_\tau - yz\rangle_\tau]$
	$\begin{cases} 3z^2 - r^2\rangle \\ 3z^2 - r^2\rangle_\tau \end{cases}$		$2^{-1/2}(xy\rangle \pm \gamma xy\rangle_\tau)$
	$\begin{cases} 2^{-1/2}(x\rangle \mp x\rangle_\tau) \\ -2^{-1/2}(y\rangle \pm y\rangle_\tau) \end{cases}$	$(\Gamma X)_3, (\Gamma X)_4$	$2^{-1/2}(x^2 - y^2\rangle \pm \gamma x^2 - y^2\rangle_\tau)$
	$\begin{cases} 2^{-1/2}(xz\rangle \pm xz\rangle_\tau) \\ 2^{-1/2}(yz\rangle \mp yz\rangle_\tau) \end{cases}$		$2^{-1}(x\rangle - y\rangle) \pm \gamma [x\rangle_\tau - y\rangle_\tau]$
Point X	2 two-dimensional representations	Line XL	1 two-dimensional representation $\gamma = \exp(ik_x a/2)$
X_1	$\begin{cases} s\rangle \\ s\rangle_\tau \end{cases}$	$(XL)_1$	$\begin{cases} s\rangle \\ \gamma s\rangle_\tau \end{cases}$
	$\begin{cases} 3z^2 - r^2\rangle \\ 3z^2 - r^2\rangle_\tau \end{cases}$		$\begin{cases} -\gamma z\rangle_\tau \\ z\rangle \end{cases}$
	$\begin{cases} xy\rangle \\ xy\rangle_\tau \end{cases}$		$\begin{cases} 3z^2 - r^2\rangle \\ \gamma 3z^2 - r^2\rangle_\tau \end{cases}$
	$\begin{cases} -2^{-1/2}(x\rangle + y\rangle) \\ 2^{-1/2}(x\rangle + y\rangle) \end{cases}$		$\begin{cases} \gamma x^2 - y^2\rangle_\tau \\ x^2 - y^2\rangle \end{cases}$
	$\begin{cases} 2^{-1/2}(xz\rangle_\tau - yz\rangle_\tau) \\ 2^{-1/2}(xz\rangle - yz\rangle) \end{cases}$		$\begin{cases} xy\rangle \\ \gamma xy\rangle_\tau \end{cases}$
X_2	$\begin{cases} z\rangle \\ - z\rangle_\tau \end{cases}$		$\begin{cases} 2^{-1/2}(x\rangle - y\rangle) \\ 2^{-1/2}\gamma(x\rangle_\tau - y\rangle_\tau) \end{cases}$
	$\begin{cases} -2^{-1/2}(x\rangle_\tau - y\rangle_\tau) \\ 2^{-1/2}(x\rangle - y\rangle) \end{cases}$		$\begin{cases} 2^{-1/2}\gamma(x\rangle_\tau + y\rangle_\tau) \\ 2^{-1/2}(x\rangle + y\rangle) \end{cases}$
	$\begin{cases} x^2 - y^2\rangle \\ x^2 - y^2\rangle_\tau \end{cases}$		$\begin{cases} 2^{-1/2}(xz\rangle + yz\rangle) \\ -2^{-1/2}\gamma(xz\rangle_\tau + yz\rangle_\tau) \end{cases}$
	$\begin{cases} 2^{-1/2}(xz\rangle_\tau + yz\rangle_\tau) \\ 2^{-1/2}(xz\rangle + yz\rangle) \end{cases}$		$\begin{cases} -2^{-1/2}\gamma(xz\rangle_\tau - yz\rangle_\tau) \\ 2^{-1/2}(xz\rangle - yz\rangle) \end{cases}$
Point P	2 two-dimensional representations	Line XP	1 two-dimensional representation $\gamma = \exp(ik_x c/4)$
P_1	$\begin{cases} s\rangle \\ s\rangle_\tau \end{cases}$	$(XP)_1$	$\begin{cases} s\rangle \\ -\gamma s\rangle_\tau \end{cases}$
	$\begin{cases} -2^{-1/2}(x\rangle_\tau + i y\rangle_\tau) \\ 2^{-1/2}(x\rangle - i y\rangle) \end{cases}$		$\begin{cases} z\rangle \\ -\gamma z\rangle_\tau \end{cases}$
	$\begin{cases} 3z^2 - r^2\rangle \\ 3z^2 - r^2\rangle_\tau \end{cases}$		$\begin{cases} \gamma x\rangle_\tau \\ y\rangle \end{cases}$
	$\begin{cases} 2^{-1/2}(xz\rangle_\tau - i yz\rangle_\tau) \\ 2^{-1/2}(xz\rangle + i yz\rangle) \end{cases}$		$\begin{cases} \gamma y\rangle_\tau \\ x\rangle \end{cases}$
P_2	$\begin{cases} z\rangle \\ - z\rangle_\tau \end{cases}$		$\begin{cases} 3z^2 - r^2\rangle \\ -\gamma 3z^2 - r^2\rangle_\tau \end{cases}$
	$\begin{cases} -2^{-1/2}(x\rangle_\tau - i y\rangle_\tau) \\ 2^{-1/2}(x\rangle + i y\rangle) \end{cases}$		$\begin{cases} \gamma yz\rangle_\tau \\ xz\rangle \end{cases}$
	$\begin{cases} xy\rangle \\ - xy\rangle_\tau \end{cases}$		$\begin{cases} \gamma xz\rangle_\tau \\ yz\rangle \end{cases}$
	$\begin{cases} x^2 - y^2\rangle \\ x^2 - y^2\rangle_\tau \end{cases}$		$\begin{cases} x^2 - y^2\rangle \\ \gamma x^2 - y^2\rangle_\tau \end{cases}$
	$\begin{cases} 2^{-1/2}(xz\rangle_\tau + i yz\rangle_\tau) \\ 2^{-1/2}(xz\rangle - i yz\rangle) \end{cases}$		$\begin{cases} xy\rangle \\ -\gamma xy\rangle_\tau \end{cases}$
Point V	4 one-dimensional representations	Line PV	2 one-dimensional representations
V_1, V_2	$2^{-1/2}(s\rangle \pm s\rangle_\tau)$	$(PV)_1, (PV)_2$	$2^{-1/2}(s\rangle \pm s\rangle_\tau)$
	$2^{-1/2}(3z^2 - r^2\rangle \pm 3z^2 - r^2\rangle_\tau)$		$2^{-1/2}(x\rangle \mp x\rangle_\tau)$
	$2^{-1/2}(z\rangle \mp z\rangle_\tau)$		$2^{-1/2}(y\rangle \pm y\rangle_\tau)$
	$2^{-1/2}(x^2 - y^2\rangle \pm x^2 - y^2\rangle_\tau)$		$2^{-1/2}(z\rangle \mp z\rangle_\tau)$
V_3, V_4	$2^{-1/2}(y\rangle \mp y\rangle_\tau)$		$2^{-1/2}(3z^2 - r^2\rangle \pm 3z^2 - r^2\rangle_\tau)$
	$2^{-1/2}(yz\rangle \pm yz\rangle_\tau)$		$2^{-1/2}(x^2 - y^2\rangle \pm x^2 - y^2\rangle_\tau)$
	$2^{-1/2}(xy\rangle \pm xy\rangle_\tau)$		$2^{-1/2}(yz\rangle \mp yz\rangle_\tau)$
			$2^{-1/2}(xy\rangle \mp xy\rangle_\tau)$
Line ΓH and LR	4 one-dimensional representations 1 two-dimensional representation $\gamma = \exp(ik_x c/4)$ for ΓH ; $\gamma = i \exp(ik_x c/4)$ for LR	Plane ΓLR	2 one-dimensional representations
$(\Gamma H)_1, (\Gamma H)_2$	$2^{-1/2}(s\rangle \pm \gamma s\rangle_\tau)$	$(\Gamma LR)_1$	$ s\rangle$
	$2^{-1/2}(z\rangle \pm \gamma z\rangle_\tau)$		$ s\rangle_\tau$
	$2^{-1/2}(x^2 - y^2\rangle \mp \gamma x^2 - y^2\rangle_\tau)$	$(\Gamma LR)_2$	$ x\rangle$
$(\Gamma H)_3, (\Gamma H)_4$	$2^{-1/2}(xy\rangle \mp \gamma xy\rangle_\tau)$		$ x\rangle_\tau$
			$ z\rangle$
$(\Gamma H)_5$	$\begin{cases} x\rangle \\ -\gamma y\rangle_\tau \end{cases}$		$ z\rangle_\tau$
	$\begin{cases} -\gamma x\rangle_\tau \\ y\rangle \end{cases}$		$ 3z^2 - r^2\rangle$
	$\begin{cases} xz\rangle \\ -\gamma yz\rangle_\tau \end{cases}$		$ xz\rangle$
	$\begin{cases} -\gamma xz\rangle_\tau \\ yz\rangle \end{cases}$		$ xz\rangle_\tau$
			$ x^2 - y^2\rangle$
			$ x^2 - y^2\rangle_\tau$
Plane LPR	2 one-dimensional representations $\gamma = -i \exp[i(k_x a/2 + k_x c/4)]$	Plane LPR	2 one-dimensional representations
$(LPR)_1$	$2^{-1/2}(s\rangle \pm \gamma s\rangle_\tau)$	$(LPR)_1$	$2^{-1/2}(s\rangle \pm \gamma s\rangle_\tau)$
	$2^{-1/2}(y\rangle \mp \gamma y\rangle_\tau)$	$(LPR)_2$	$2^{-1/2}(x\rangle \mp \gamma x\rangle_\tau)$
	$2^{-1/2}(3z^2 - r^2\rangle \pm \gamma 3z^2 - r^2\rangle_\tau)$		$2^{-1/2}(z\rangle \pm \gamma z\rangle_\tau)$
	$2^{-1/2}(x^2 - y^2\rangle \mp \gamma x^2 - y^2\rangle_\tau)$		$2^{-1/2}(xz\rangle \mp \gamma xz\rangle_\tau)$
	$2^{-1/2}(yz\rangle \mp \gamma yz\rangle_\tau)$		$2^{-1/2}(x^2 - y^2\rangle \mp \gamma x^2 - y^2\rangle_\tau)$
			$2^{-1/2}(yz\rangle \mp \gamma yz\rangle_\tau)$
			$2^{-1/2}(xy\rangle \pm \gamma xy\rangle_\tau)$

TABLE I (continued)

2 one-dimensional representations		
Plane ΓPX	$\gamma = \exp[i(k_x a/2 + k_z c/4)]$	
$(\Gamma PX)_1$	$2^{-1/2}(s\rangle \pm \gamma s\rangle_r)$	$2^{-1/2}(x\rangle \pm \gamma y\rangle_r)$
$(\Gamma PX)_2$	$2^{-1/2}(y\rangle \pm \gamma x\rangle_r)$	$2^{-1/2}(z\rangle \pm \gamma z\rangle_r)$
	$2^{-1/2}(3z^2 - r^2\rangle \pm \gamma 3z^2 - r^2\rangle_r)$	$2^{-1/2}(xz\rangle \pm \gamma yz\rangle_r)$
	$2^{-1/2}(x^2 - y^2\rangle \mp \gamma x^2 - y^2\rangle_r)$	$2^{-1/2}(yz\rangle \pm \gamma xz\rangle_r)$
	$2^{-1/2}(xy\rangle \pm \gamma xy\rangle_r)$	
2 one-dimensional representations		
Plane ΓLX	$\gamma = \exp(ik_x a/2)$	
$(\Gamma LX)_1$	$2^{-1/2}(s\rangle \pm \gamma s\rangle_r)$	$2^{-1/2}(x\rangle \pm \gamma x\rangle_r)$
$(\Gamma LX)_2$	$2^{-1/2}(y\rangle \pm \gamma y\rangle_r)$	$2^{-1/2}(z\rangle \mp \gamma z\rangle_r)$
	$2^{-1/2}(3z^2 - r^2\rangle \pm \gamma 3z^2 - r^2\rangle_r)$	$2^{-1/2}(xz\rangle \mp \gamma xz\rangle_r)$
	$2^{-1/2}(x^2 - y^2\rangle \pm \gamma x^2 - y^2\rangle_r)$	$2^{-1/2}(yz\rangle \mp \gamma yz\rangle_r)$
	$2^{-1/2}(xy\rangle \pm \gamma xy\rangle_r)$	

$\tau = (a/2, 0, c/4)$. The basic primitive vectors for the reciprocal lattice are $\mathbf{b}_1 = 2\pi(0, 1/a, 1/c)$, $\mathbf{b}_2 = 2\pi(1/a, 0, 1/c)$, $\mathbf{b}_3 = 2\pi(1/a, 1/a, 0)$, and all the reciprocal lattice vectors are written as $\mathbf{k}_n = n_1\mathbf{b}_1 + n_2\mathbf{b}_2 + n_3\mathbf{b}_3$, where n_1, n_2, n_3 are integers. The Brillouin zone for the white tin structure is shown in Fig. 2.

Several fundamental distances in the Brillouin zone are given below:

$$\Gamma L = (2\pi/a) = 0.5713(1/a_0),$$

$$\Gamma X = 0.7071(2\pi/a) \text{ (the minimal boundary distance from the zone center),}$$

$$\Gamma H = \Gamma R = (1/2)(c/a + a/c)(2\pi/a) = 1.1893(2\pi/a) \text{ (the maximal distance),}$$

$$\Gamma P = 1.1576(2\pi/a),$$

$$\Gamma V = 1.0441(2\pi/a),$$

$$LR = \Gamma W = (1/2)(a/c - c/a)(2\pi/a) = 0.6438(2\pi/a), \text{ and}$$

$$RP = 0.7579(2\pi/a).$$

A group-theoretical analysis for the symmetry of white tin has been presented earlier.¹⁸⁻²¹ Here, in

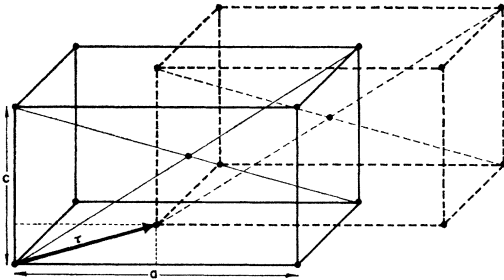


FIG. 1. The white tin structure.

¹⁸ S. Mase, J. Phys. Soc. Japan 14, 1538 (1959).

¹⁹ M. Miasek and M. Suffczynski, Bull. Acad. Polon. Sci., Ser. Math. Astron. Phys. 9, 477 (1961); we point out that matrices for representations P_1 and P_2 have to be taken as the complex

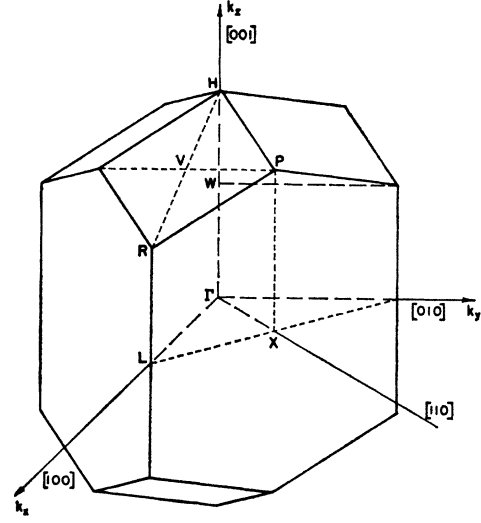


FIG. 2. The Brillouin zone for white tin structure.

Table I, the group theoretical classification for atomic functions s , p , and d is given. Such a classification is very useful in band structure calculations. The notation for the Bloch functions used here is illustrated in the following example:

$$|x\rangle = N^{-1/2} \sum_j \exp(i\mathbf{k} \cdot \mathbf{r}_j) \psi_{n, l=1, m=1}(\mathbf{r} - \mathbf{r}_j),$$

$$|x\rangle_r = N^{-1/2} \sum_j \exp(i\mathbf{k} \cdot \mathbf{r}_j) \psi_{n, l=1, m=1}(\mathbf{r} - \mathbf{r}_j - \boldsymbol{\tau}),$$

where $\psi_{nlm}(\mathbf{r})$ are the atomic functions. Where two signs appear in the formulas, the upper sign refers to the representation written first, the lower sign to the one written second.

III. METHOD AND RESULTS OF CALCULATIONS

The wave functions of electrons in the conduction band are assumed to be orthogonalized plane waves:

$$\psi^{\alpha j}(\mathbf{k}; \mathbf{r}) = \phi^{\alpha j}(\mathbf{k}; \mathbf{r}) - \sum_c c(\psi_c^{\alpha j}, \phi^{\alpha j}) \psi_c^{\alpha j}(\mathbf{k}; \mathbf{r}). \quad (1)$$

Here, $\phi(\mathbf{k}; \mathbf{r})$ is taken as a linear combination of the symmetrized plane waves; ψ_c are the Bloch functions for core states. The index α denotes a row of the irreducible representation. The index is later omitted; it must be remembered that the basis functions of the given irreducible representations are used exclusively in the following.

The Schrödinger equation for the conduction electrons in crystal is $H\psi = E\psi$, where $H = H_0 + V$ and $H_0 = T + V(0)$ is the free-electron Hamiltonian. $V(0)$ is the space average of the crystal potential; $V = V_c$

conjugate of the matrices listed there; 9, 483 (1961); we point out that matrices for B_j operations must be multiplied by γ^* .

²⁰ M. Suffczynski, Bull. Acad. Polon. Sci., Ser. Math. Astron. Phys. 9, 489 (1961).

²¹ M. Miasek, Bull. Acad. Polon. Sci., Ser. Math. Astron. Phys. 10, 39 (1962).

— $V(0)$, where V_c is the total crystal potential. We can write

$$(H_0 + V + V_R)\phi = E\phi, \quad (2)$$

where

$$V_R\phi = \sum_c (E - E_c) (\psi_c, \phi) \psi_c. \quad (3)$$

V_R is treated as the repulsive potential obtained as a consequence of the orthogonalization of the plane waves to the functions of core states.²²⁻²⁶

The choice of V_R is made by a variational procedure in such a way that the uniquely determined function ϕ consists, hopefully, of only a few plane waves. Then, $V + V_R$ is treated as the perturbation. The energy to second order is given by

$$E = W_0 + [\langle S_0 | V | S_0 \rangle + \sum_c (W_0 - E_c) |\langle \psi_c | S_0 \rangle|^2] \\ \times [1 + \sum_c |\langle \psi_c | S_0 \rangle|^2] - \sum_j' (W_j - W_0)^{-1} \langle S_j | V | S_0 \rangle \\ + \sum_c (W_0 - E_c) \langle \psi_c | S_0 \rangle \langle S_j | \psi_c \rangle|^2. \quad (4)$$

S_0 and S_j are the symmetrized plane waves in the expansion of $\phi(\mathbf{k}; \mathbf{r})$.

$$S_j = (N\Omega_0)^{-1/2} \sum_s a_s^{(j)} \exp[i(\mathbf{k} + \mathbf{k}_s^{(j)}) \cdot \mathbf{r}], \quad (5)$$

where Ω_0 is the volume of the unit cell; $a_s^{(j)}$ are obtained by group theoretical considerations; $\mathbf{k}_s^{(j)}$ are the reciprocal lattice vectors given by the symmetry group for given \mathbf{k} . $\mathbf{k} + \mathbf{k}_s^{(j)}$ are of the same length for every s . $W_j = V(0) + (\hbar^2/2m)|\mathbf{k} + \mathbf{k}_s^{(j)}|^2$ is the free-electron energy corresponding to the symmetrized plane wave S_j . The ψ_c are the functions of core states assumed to be of the form

$$\psi_c = \psi_{nl} = N^{-1/2} \sum_m \sum_\omega c_m(\omega) \\ \times \sum_j \exp(i\mathbf{k} \cdot \mathbf{r}_j) \psi_{nlm}(\mathbf{r} - \mathbf{r}_j - \mathbf{t}_\omega), \quad (6)$$

where ψ_{nlm} are the atomic functions; the \mathbf{t}_ω are two basis vectors in the unit cell; and $c_m(\omega)$ are obtained from group theoretical considerations. The functions ψ_c are assumed orthogonal and normalized; they describe the states from 1s to 4d in white tin.

The matrix elements between symmetrized plane waves and core functions are given by

$$\langle S_j | \psi_c \rangle = [4\pi/(2l+1)]^{1/2} \\ \times \sum_s \sum_m a_s^{(j)*} [c_m^{(1)} + c_m^{(2)} \exp(-i\mathbf{k}_s^{(j)} \cdot \boldsymbol{\tau})] \\ \times A_{nl}(|\mathbf{k}_s^{(j)}|) * Y_{lm}(\theta_{\mathbf{k}_s, \boldsymbol{\tau}}). \quad (7)$$

Here, A_{nl} are the orthogonalization coefficients,²⁷

$$A_{nl}(k) = \Omega_0^{-1/2} i^l [4\pi(2l+1)]^{1/2} \int r j_l(kr) P_{nl}(\tau) dr, \quad (8)$$

where $j_l(kr)$ is a spherical Bessel function.

²² E. Antončík, Czechoslov. J. Phys. **4**, 439 (1954); **10**, 22 (1960); J. Phys. Chem. Solids **10**, 314 (1959).

²³ J. C. Phillips, Phys. Rev. **112**, 685 (1958).

²⁴ J. C. Phillips and L. Kleinman, Phys. Rev. **116**, 287, 880 (1959); **117**, 460 (1960); **118**, 1153 (1960).

²⁵ M. H. Cohen and V. Heine, Phys. Rev. **122**, 1821 (1961).

²⁶ B. J. Austin, V. Heine, and L. J. Sham, Phys. Rev. **127**, 276 (1962).

²⁷ T. O. Woodruff, in *Solid State Physics*, edited by F. Seitz and D. Turnbull (Academic Press Inc., New York, 1955), Vol. 4, p. 314.

The crystal potential can be written as

$$V_c = \sum_j [V_a(\mathbf{r} - \mathbf{r}_j) + V_a(\mathbf{r} - \mathbf{r}_j - \boldsymbol{\tau})],$$

where V_a is the potential in one atomic cell. The matrix elements of the V potential between symmetrized plane waves are given by

$$\langle S_j | V | S_0 \rangle = \sum_s \sum_l a_l^{(0)} a_s^{(j)*} [1 + \exp\{i(\mathbf{k}_l^{(0)} - \mathbf{k}_s^{(j)}) \cdot \boldsymbol{\tau}\}] \\ \times V_a(\mathbf{k}_l^{(0)} - \mathbf{k}_s^{(j)}) - V(0)\delta_{j0}, \quad (9)$$

and

$$V_a(\mathbf{k}) = \Omega_0^{-1} \int \exp(i\mathbf{k} \cdot \mathbf{r}) V_a(\mathbf{r}) d\mathbf{r}. \quad (10)$$

The calculations have been performed for different choices of potential. In the first instance $V_a(\mathbf{r})$ consisted of the Coulomb part for all electronic states in tin and the exchange part as given by Slater free-electron approximation.²⁸⁻³⁰ Both in obtaining the potential, and in the final formula for the energy, we have used the core eigenfunctions and eigenvalues given by Herman and Skillman. The Fourier coefficients of the atomic potential as given by (10) are tabulated in the second column of the Table II. $V(0)$ was inferred from the renormalization of $V(0)$ for grey tin and it is equal to -2.63 Ry.³¹ In this first approximation, the results obtained did not in fact confirm the supposition that the conduction electrons should be nearly free. The energy gaps between levels which were degenerate in free-electron model, were very large (up to 0.65 Ry). The convergence of the method was poor but one must point out here that the large energy gaps are mainly determined by first-order contribution to the energy $E^{(1)}$ and the second-order term $E^{(2)} \sum_c |\langle S_0 | \psi_c \rangle|^2$. The negative second-order contributions have negligible influence on the energy gaps.

In our second treatment, the potential is chosen in such a way that the exchange part of the potential contains screening.³² The new Fourier coefficients of potential are tabulated in the third column of the Table II. $V(0)$ was calculated and its value is -2.39 Ry.

Considering the new potential one must take into

TABLE II. Fourier coefficients of atomic potential (in rydbergs); $\mu = a/c$.

$(a/2\pi)\mathbf{k}_n$	$V_a(\mathbf{k}_n)$	
	unscreened exchange	screened exchange
2, 0, 0	-0.5051	-0.4533
1, 0, μ	-0.4859	-0.4388
2, 2, 0	-0.3651	-0.3403
2, 1, μ	-0.3573	-0.3335
3, 0, μ	-0.2920	-0.2763
0, 0, 2 μ	-0.2779	-0.2637

²⁸ J. C. Slater, Phys. Rev. **81**, 385 (1951).

²⁹ T. O. Woodruff, Phys. Rev. **103**, 1159 (1956).

³⁰ F. Herman, Phys. Rev. **93**, 1214 (1954).

³¹ F. Bassani (private communication).

³² J. E. Robinson, F. Bassani, R. S. Knox, and J. R. Schrieffer, Phys. Rev. Letters **9**, 215 (1962).

account that the core eigenvalues and eigenfunctions should be computed in this potential. At the present stage we did not perform the laborious recalculations of the core eigenvalues and eigenfunctions, but in order to obtain the final results, which would approximate the results given by self-consistent treatment, we used the following considerations. We may assume that the core eigenfunctions are not really seriously changed by the change of potential, so we may still work with the same orthogonalization coefficients as for the first choice of potential. But we must not neglect the changes of eigenvalues of the core states. The effect of screening is that the new negative core eigenvalues are $E_c' = E_c + \Delta E_c$, where ΔE_c is a positive correction. In the formula for the energy the core eigenvalues appear in expressions

$$W_0 - E_c = V(0) + T_0 - E_c. \quad (11)$$

When we now put the new energies into these expressions we get

$$V(0) + T_0 - E_c - \Delta E_c = [V(0) - \Delta E_c] + T_0 - E_c. \quad (12)$$

On the average, the effect of the new core eigenvalues is such as to make $V(0)$ larger in magnitude and leave the E_c the same as before. The new $V(0)$ should be larger in magnitude than 2.39.

To establish this new $V(0)$ we used the following procedure. We found the energies of the levels Γ_1^+ , Γ_1^- , Γ_4^- , Γ_5^+ as a function of $V(0)$. The appropriate curves giving the energies of Γ_1^- , Γ_4^- , Γ_5^+ states relative to Γ_1^+ energy are shown in Fig. 3.

We may expect the Fermi energy in white tin nearly to be the same as in free-electron approximation, i.e., $E_F = 2.31(2\pi/a)^2 = 0.754$ Ry relative to the lowest Γ_1^+ level. We assumed also that the existence of electrons around the zone center in the fifth Brillouin zone, as it was predicted by free-electron model, is really well confirmed by the de Haas-van Alphen experiment. From

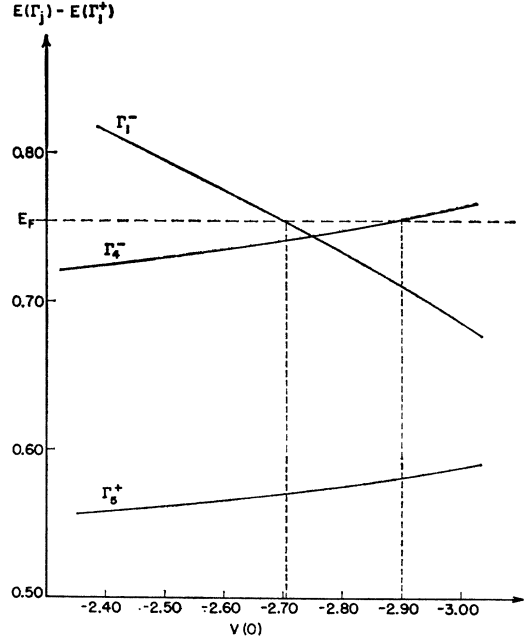


FIG. 3. The dependence $E(\Gamma_j) - E(\Gamma_1^+)$ on $V(0)$; Γ_j corresponds to Γ_1^- , Γ_4^- , Γ_5^+ .

Fig. 3 we see that the second assumption is true only if $V(0)$ is in the limited interval between -2.71 and -2.90 Ry. From this semiempirical fitting we obtain a possible value of $V(0)$ really larger than 2.39.

Unfortunately, by this procedure, we could not find a unique value of $V(0)$. For the calculations with screened potential, two values of $V(0)$ were chosen for discussion. One is $V(0) = -2.72$ Ry, from the region where $E(\Gamma_4^-) < E(\Gamma_1^-)$; the other one is -2.80 Ry, where $E(\Gamma_4^-) > E(\Gamma_1^-)$.

The results of the calculations for the points of high symmetry in Brillouin zone are given in Table III; the

TABLE III. Energies at symmetry points (in rydbergs).

	$E(\mathbf{k})$ $V(0) = -2.72$	$E(\mathbf{k})$ $V(0) = -2.80$	$E(\mathbf{k}) - E(\Gamma_1^+)$ $V(0) = -2.72$	$E(\mathbf{k}) - E(\Gamma_1^+)$ $V(0) = -2.80$	$E(\mathbf{k}) - E(\Gamma_1^+)$ free-electrons
Γ_1^+	-1.672	-1.763	0.000	0.000	0.000
Γ_1^-	-0.928	-1.030	0.744	0.733	0.653
Γ_4^-	-0.930	-1.016	0.742	0.747	0.653
Γ_5^+	-1.100	-1.186	0.572	0.577	0.653
L_2	-1.342	-1.440	0.330	0.323	0.326
L_3	-1.355	-1.440	0.317	0.323	0.326
L_2'	-0.559	-0.649	1.113	1.114	1.097
X_1	-1.523	-1.615	0.149	0.148	0.163
X_2	-0.926	-1.014	0.746	0.749	0.816
X_1'	-0.756	-0.851	0.916	0.932	0.816
P_1	-1.224	-1.323	0.448	0.440	0.437
P_2	-1.256	-1.341	0.416	0.422	0.437
$H_1^{(1)}$	-1.230	-1.315	0.442	0.448	0.458
$H_1^{(2)}$	-1.184	-1.286	0.488	0.477	0.458
H_2	-1.205	-1.303	0.467	0.460	0.458
H_5	-1.223	-1.308	0.449	0.455	0.458
$W_5^{(1)}$	-0.837	-0.923	0.835	0.840	0.788
$W_5^{(2)}$	-0.985	-1.072	0.687	0.691	0.788

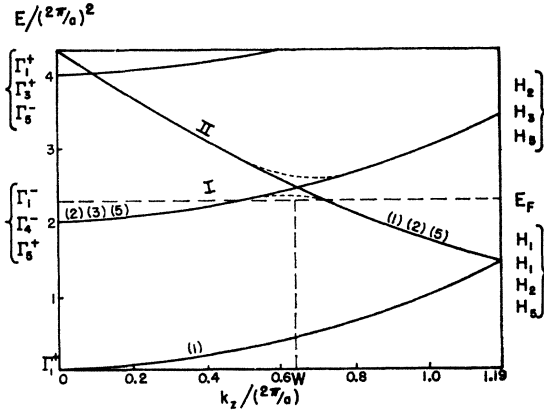


FIG. 4. The energy bands in empty lattice for [001] direction; the dashed curves show expected behavior of the bands; E_F -Fermi level.

energies are in rydbergs. The new results show that the deviation from the free-electron model is not very large. The maximal energy gap is about 0.17 Ry. In this case the convergence of the method is also very good. In the formula for the energy all symmetrized plane waves S_j with the energies up to $13.44(2\pi/a)^2$ have been included. The negative second-order contributions were, in magnitude, less than 0.04 Ry. It is possible that in our first approximation the use of a long-range (unscreened) potential was responsible for the large energy gaps. The use of screened exchange seems to solve the problem for the present but we wish to notice here that even it may be overscreened.³² The screened exchange appears to give reasonable results for substances with large dielectric constant, as for example, AgCl.³³ It is also of interest to note that in calculations with unscreened exchange, the arrangement of the Γ levels is such that the lowest level is Γ_1^+ of pure s symmetry, then Γ_1^- of s and d symmetry, Γ_5^+ of p symmetry and Γ_4^- of d symmetry. In the calculations with screened exchange the next level to the lowest Γ_1^+ is now Γ_5^+ , which is quite distinctly separated from Γ_1^- and Γ_4^- . Such an arrangement of levels seems to be quite reasonable as we remember that the valence electrons in the atomic tin are just $5s$ and $5p$ electrons.

IV. DISCUSSION AND FINAL REMARKS

The above results cannot yet explain all the details of the Fermi surface in white tin, but some indications concerning the Fermi surface close to the points of high symmetry can be inferred. In the following discussion it is assumed that the Fermi energy is the same as in the free-electron model. As established in the case of the other polyvalent metals, such an assumption is reasonable. By fitting $V(0)$, the problem of existence of electrons at the zone center is already solved according to

³³ F. Bassani, W. B. Fowler, and R. S. Knox (private communication).

free-electron model. Furthermore, a very important implication may be obtained for the second Brillouin zone. In the free-electron model a region of holes existed close to the point W along the [001] direction. But even from this model one can conclude that the holes may not exist there. In Fig. 4 the band structure for the empty lattice is shown for the [001] direction. It is seen that two crossing lines I and II both belong to the same representations $(\Gamma H)_2$ and $(\Gamma H)_5$. As a result of the repulsion of the states belonging to the same representation, the bands should have a form similar to the one shown by the dashed curve. It is obvious that the possibility exists of having one of these curves below the Fermi level.

The results of the calculations are that the first line in the ΓH direction is a line joining Γ_1^+ and the lowest H -level $H_1^{(1)}$. The next possible line, according to symmetry considerations, is the line joining Γ_5^+ and H_5 . Γ_5^+ is now about 0.08 Ry lower relative to the same free-electron level, so the line joining Γ_5^+ with H_5 should lie lower relative to the Fermi level. This is confirmed by a calculation of the energy for the W_5 representation. The lower energy of the W_5 level relative to Γ_1^+ is about 0.69 Ry. It is about 0.06 Ry below the Fermi energy. This provides strong confirmation of the fact that the two first Brillouin zones for white tin structure are completely occupied by electrons.

For the direction [110] the calculations confirm the Gold and Priestley supposition that at point X in the fourth Brillouin zone a region of holes may not exist. This problem must be very carefully checked because the calculated level for the X_2 representation really lies below the free-electron Fermi energy but very close to it.

For the other points of high symmetry agreement exists between the prediction of a free-electron model and the calculations.

To obtain the whole picture of the Fermi surface one must calculate the energy at many other points in the Brillouin zone. From the results given above, one may find the state-independent lowest Fourier coefficients of the pseudopotential. Then, using the pseudopotential method with only a few OPW's it should, in principle, be possible to find the whole Fermi surface for white tin.

ACKNOWLEDGMENTS

The author wishes to express warm thanks to Dr. F. Bassani for providing the computed Fourier coefficients of potential and orthogonalization coefficients and for valuable suggestions and discussions; to Dr. F. Herman and Dr. S. Skillman and also to Dr. D. Mayers for the Hartree-Fock atomic functions; to Professor R. Knox for many helpful discussions; and to Dr. A. V. Gold for useful suggestions concerning white tin.

It is a pleasure to thank Professor D. L. Dexter for the generous hospitality extended to me at the University of Rochester.